

Preparation and structure of the electro-deposited Ni-Mo alloys with polymers

M. Karolus*, J. Niedbała, E. Rówiński, E. Łągiewka, A. Budniok

Institute of Material Science, University of Silesia,
ul. Bankowa 12, 40-007 Katowice, Poland

* Corresponding author: E-mail address: karolus@us.edu.pl

Received 15.11.2005; accepted in revised form 15.04.2006

Materials

ABSTRACT

Purpose: The aim of the paper is presentation the process of forming the Ni-Mo electrodeposited layers with polypyrrole, polytiophne and polyethylene.

Design/methodology/approach: There are three ways of polymerization and layer deposition.

Findings: In case of polytiophen + Ni-Mo – there is observed process of electropolymerization and Ni-Mo electrodeposition in the cathodic process. In case of polypyrrole + Ni-Mo – there is observed two-step process: electropolymerization in the anodic process and Ni-Mo electrodeposition in the cathodic process. So the composite is forming when the electrodes have worked alternately as the anode and as the cathode. In case of polyethylene + Ni-Mo – there is observed process of Ni-Mo electrodeposition with grains of polyethylene in the cathodic process. From structural analyses by X-ray diffraction it was noticed that the solid solution of Mo in Ni is forming. The unit cell parameters of solid solution are slightly changing with the increasing of molybdenum contents in the alloy from the value 3.57 to 3.61 Å. In case of all polymers, the crystallite size calculated basing on the Williamson-Hall theory is about 5 - 6 nanometers.

Practical implications: The codeposition of alloys with polymers or polymerisation with alloys codeposition has created new opportunities in the preparation of novel composite materials. Conductive polymers have been investigated for use as the electrode materials for a number of applications including rechargeable batteries, electrochemical sensors etc. Electrochemical method described in this paper is unique in that it can be used for processing ceramics, polymers, metals, composites and hybrid materials.

Originality/value: Using the electropolymerization and electrodeposition processes in preparation of the composites.

Keywords: Composites; Engineering polymers; Nanomaterials; X-ray diffraction; Auger electrons

1. Introduction

Electrolytic nickel and nickel-molybdenum alloy are characterized by good corrosion and heat resistance and electrochemical activity towards cathodic hydrogen evolution and anodic oxygen evolution. They are also used as protection covers for elements working in aggressive environments [1-5]. Electrodeposition techniques have evolved into an important branch of surface engineering. Electrodeposition is unique in that it can be used for processing ceramics, polymers, metals, composites and hybrid materials [6-10]. Important advantages

gained in using electrochemical method have stimulated by accelerated growth in the development and application of electrodeposition.

The codeposition of alloys with polymers or polymerisation with alloys codeposition has created new opportunities in the preparation of novel composite materials. Conductive polymers have been investigated for use as the electrode materials for a number of applications including rechargeable batteries, electrochemical sensors etc. [11-12]. The conductivity of doped conducting polymers can be attributed to the delocalisation of π -conjugated systems. Among conductive polymers, pyrrole (PPy)

and polythiophene (PTH) have been of interest due to their high electrical conductivity, good environmental stability and the possibility of their applications in emerging technologies [13-15]. Although polypyrrole have been known for over 50 years, interest in these materials has greatly increased in the past decade because polypyrroles when doped intrinsically electrically conductive. Polypyrrole can be synthesized both chemically [16] and electrochemically [17]. Aqueous electropolymerization has several advantages over the traditional coating techniques. It combines the formation of the polymer and its deposition on the substrate in one process. Because of this, a lot of work has been done in the synthesis of polypyrrole using the electrochemical technique. The nature of the working electrode plays an important role in the synthesis of polypyrrole. It is important that the working electrode does not oxidize concurrently with the monomer. For this reason polypyrrole was synthesized using an inert platinum or gold electrode [18]. But late, polypyrrole has been synthesized on various substrates like iron [19], steel [20], aluminium, brass, mild steel [21] and zinc. It has also been copolymerised extensively with polyaniline [22]. Polypyrrole has been doped with anions derived from oxalic acid [23] and hexacyanoferrate [24]. Use also the incorporation of dispersed microparticles Pt or Cu [25,26].

Abdel Hamid et al. [27] have reported that Ni-polyethylene (Ni-PE) can be electrodeposited from nickel solution with particles PE. The incorporation of PE in the Ni- deposit improves the microhardnes, the wear as well as corrosion resistance of the deposit.

2. Material

2.1. Electrolytical obtaining of Ni-Mo layers with polypyrrole Ni-Mo+Ppy

Electrolytical Ni-Mo+PPy layers were deposited from a mixture of bath (1) and (2) in relation 1:1. The bath composition is as follows: (1) 0,035 M Na_2MoO_4 ; 0,75 M NiSO_4 ; 0,45 M $\text{Na}_3\text{C}_6\text{H}_5\text{O}_7$, pH 6,0-7,0 [24,25], (2) 0,05 M NaClO_4 ; 0,1 M pyrrole ($\text{C}_4\text{H}_5\text{N}$) (99,9% Aldrich). Pyrrole was freshly distilled and next solubilized in NaClO_4 solution.

The layers were plated on steel substrate (S235JR, 4 cm^2), which was prepared by mechanical polishing, chemical etching in 1:1 HCl solution for 5 min. and electrochemical etching in sodium gluconate ($\text{C}_6\text{H}_{11}\text{NaO}_7$) solution. The other side of the plates was covered with non-conductive resin. The layers were electrodeposited at room temperature. Electrochemical studies were conducted in a three-electrode thermostatic, electrolytic vessel with VOLTAMASTER PG 201 from RADIOMETER. The reference electrode was calomel electrode, cathode and anode was steel substrate and we obtaining two coatings trough use reversion of the process conditions. In case of polypyrrole + Ni-Mo – there is observed two-step process: electropolymerization in the anodic process and Ni-Mo electrodeposition in the cathodic process. So the composite is forming when the electrodes have worked alternately as the anode and as the cathode. The cyclic chronovoltamperometric curve recorded in the range from -1,8 to +1,0 V was used to determine the potential and current density

of electrodeposition and electropolymerization processes. For the current reversion method a value $j = \pm 10 \text{ mA/cm}^2$, the impulse time $t = 90 \text{ s}$, complete charge $Q=720 \text{ C}$ was chosen. The potentials of electropolymerization and electrodeposition at potential reversion method were: +0.6 V /-1.2 V, +0.7 V /-1.4 V, +0.8 V /-1.6 V (the time of cathodic and anodic impulse was 3 min.), the complete time was 30 min. The example of the X-ray diffraction pattern obtained for the sample “+0.7 V /-1.4 V” is presented on the Fig.1.

2.2. Electrolytical obtaining of Ni-Mo layers with polythiophene Ni-Mo+PTh

Electrolytical layers with polythiophene (PTh) were deposited from a mixture of bath (1) and (2) in relation 1:1. The bath composition is as follows: (1) 0,035 M Na_2MoO_4 ; 0,75 M NiSO_4 ; 0,45 M $\text{Na}_3\text{C}_6\text{H}_5\text{O}_7$, pH 6,0-7,0 [24,25], (2) 0,025 M HClO_4 ; 0,1 M thiophene ($\text{C}_4\text{H}_4\text{S}$) (99,9% Aldrich). Thiophene was freshly distilled and next solubilized in HClO_4 solution.

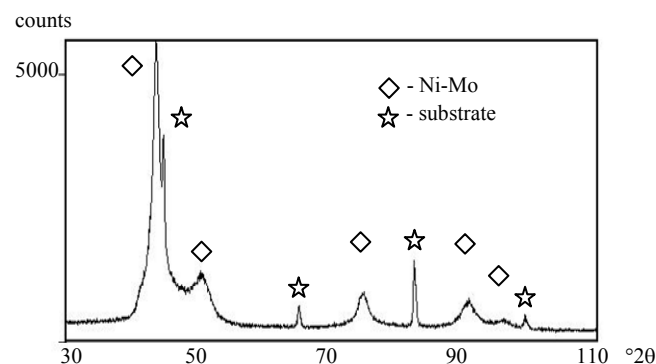


Fig. 1. The example of the X-ray diffraction pattern obtained for the sample “+0.7 V /-1.4 V”.

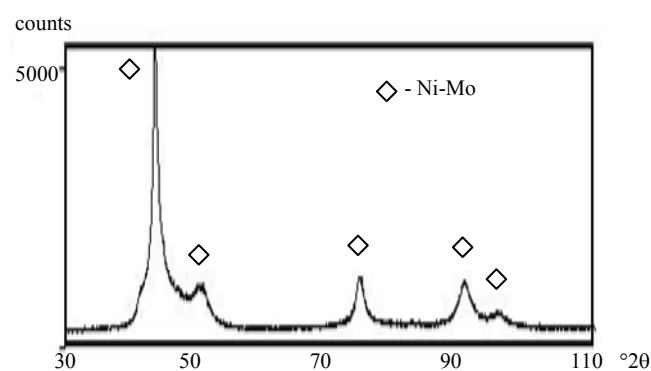


Fig. 2. The example of the X-ray diffraction pattern obtained for the sample “150 mA/cm^2 ”.

The layers were plated on steel substrate (S235JR, 4 cm^2), which was prepared by mechanical polishing, chemical etching in 1:1 HCl solution for 5 min. and electrochemical etching in sodium

gluconate $C_6H_{11}NaO_7$ solution. The other side of the plates was covered with non-conductive resin. In case of polytiophen + Ni-Mo – there is observed process of electropolymerization and Ni-Mo electrodeposition in the cathodic process. The layers were electrodeposited at room temperature under galvanostatic conditions ($j_{dep} = 25, 50, 100, 150$ and 200 mA/cm^2), complete charge $Q = 720 \text{ C}$ was chosen. The example of the X-ray diffraction pattern obtained for the sample “150 mA/cm^2 ” is presented on the Fig.2.

2.3. Electrolytical obtaining of Ni-Mo layers with polyethylene Ni-Mo+PE_(Ni)

Ni-Mo+PE_(Ni) composite layers were electrodeposited from nickel-molybdenum bath [mol/dm^3]: Na_2MoO_4 0,035; $NiSO_4$ 0,75; $Na_3C_6H_5O_7$ 0,45 containing polyethylene grain suspension [10 g/dm^3] (PELD d = 0,91 – 0,925 g/cm^3). The PELD grain were initially activate and next nickeled by electroless method in a bath of composition [mol/dm^3]: 0,19 M $NiSO_4$; 0,47 M NaH_2PO_2 (T = 374 K, t = 60min.).

The layers were plated on steel substrate (S235JR, 4 cm^2), which was prepared by mechanical polishing, chemical etching in 1:1 HCl solution for 5 min. and electrochemical etching in sodium gluconate $C_6H_{11}NaO_7$ solution. The other side of the plates was covered with non-conductive resin. In case of polyethylene + Ni-Mo – there is observed process of Ni-Mo electrodeposition with grains of polyethylene in the cathodic process.

The Ni-Mo+PE_(Ni) coatings were electrodeposited at room temperature under galvanostatic conditions ($j_{dep} = 20, 200 \text{ mA/cm}^2$), complete charge $Q = 720 \text{ C}$ was chosen.

The example of the X-ray diffraction pattern obtained for the sample “200 mA/cm^2 ” is presented on the Fig.3.

3. Experimental methods and discussion

3.1. X-ray diffraction

The X-ray diffraction patterns were measured at room temperature using Philips Diffractometer PW 1130 for all samples. The copper radiation ($\lambda_{K\alpha} = 1.5418 \text{ \AA}$), graphite monochromator on the diffracted beam, the step scanning mode in a range of 30 - 110° 2 θ with the step of 0.04° 2 θ and counting time of 4 s were used.

After analysis of the X-ray diffraction patterns (Fig. 1 – 3) it is clear that the solid solution of molybdenum in nickel is forming in all obtained samples. The calculated values of the unit cell parameters of all studied alloys are presented in the table 1. It was noticed that, in general, the values of unit cell parameters does not depend on the type of electrodeposition method. These values also slightly depend on the values of potentials and current densities. In comparison, in earlier experiments carried out on the electrodeposited Ni-Mo alloys [28, 29, 30, 31] it had been shown that the values of the unit cell parameters were strongly depended on the current densities and these values were changed from 3.541 to 3.622 \AA . So, it is possible to notice that the presence of

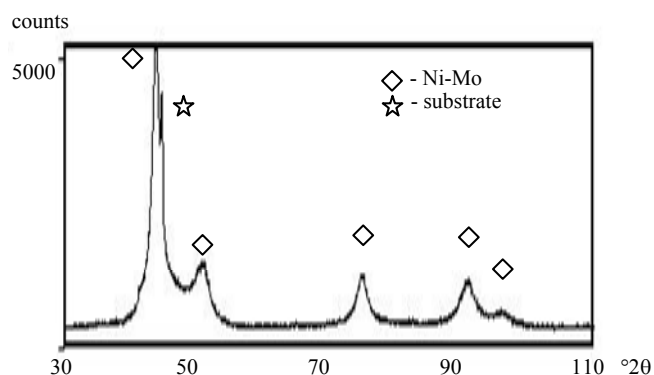


Fig. 3. The example of the X-ray diffraction pattern obtained for the sample “200 mA/cm^2 ”.

the polymers in the electrolyte hampers the process of the layer electrodeposition. In particular the presence of the polymers decreases the content of molybdenum in the solution [28, 29, 30, 31].

Table 1

The values of the unit cell parameters [\AA] (accuracy of $\pm 10^{-4} [\text{\AA}]$)

Sample	Unit cell parameters [\AA]
Ni-Mo layers with polypyrrole (Ni-Mo+PPy)	
+0.6 / -1.2 V/cm^2	3.6062
+0.7 / -1.4 V/cm^2	3.5868
+0.8 / -1.6 V/cm^2	3.6003
Ni-Mo layers with polytiophene (Ni-Mo+PTh)	
25 mA/cm^2	3.5976
50 mA/cm^2	3.6049
100 mA/cm^2	3.6053
150 mA/cm^2	3.6107
200 mA/cm^2	3.5998
Ni-Mo layers with polyethylene (Ni-Mo+PE _(Ni))	
20 mA/cm^2	3.6003
200 mA/cm^2	3.5738

Table 2

The values of the crystallite size [\AA] and the lattice distortion [%] (accuracy of 15 %)

Sample	Crystallite size [\AA]	Lattice distortion [%]
Ni-Mo layers with polypyrrole (Ni-Mo+PPy)		
+0.6 / -1.2 V/cm^2	62	1.3
+0.7 / -1.4 V/cm^2	50	1.6
+0.8 / -1.6 V/cm^2	50	1.6
Ni-Mo layers with polytiophene (Ni-Mo+PTh)		
25 mA/cm^2	48	1.5
50 mA/cm^2	62	1.3
100 mA/cm^2	50	1.6
150 mA/cm^2	60	1.4
200 mA/cm^2	62	1.6
Ni-Mo layers with polyethylene (Ni-Mo+PE _(Ni))		
20 mA/cm^2	54	1.8
200 mA/cm^2	55	1.5

The broadening of the diffraction lines points out that the crystallite size of the obtained layers is in a range of 5 – 6 nanometers. Basing on the classical Williamson–Hall theory [32] the crystallite size and the lattice distortion of studied alloys were calculated and the results are presented in the table 2. During calculations the diffraction lines 111, 200, 220, 311 and 222 were tested. In comparison, in earlier experiments carried out on the electrodeposited Ni-Mo alloys [28, 29, 30, 31] it had been shown that the values of the crystallite size were depended on the current densities and these values were in a range of 2 – 7 nm (except of the sample “5 mA/cm²” where the crystallite size is 23 nm).

3.2. Auger experiment

Measurements performed for chosen alloys (Ni-Mo layers with polythiophene (Ni-Mo+PTh) – 50 and 200 mA/cm² and Ni-Mo layers with polyethylene (Ni-Mo+PE_(Ni)) – 200 mA/cm²) were provided in the vacuum system of on SP-2000 1/M type with the help of spectrometers Auger SEA 02 and PHI 5700/660 [33, 34]. The clean surfaces of the samples were obtained removing C and O atoms by means of in situ method, was additional etched by Ar⁺ beam with particle energy E_j = 4 keV and density of current 0.72 μAmm⁻².

In Fig. 4 we have presented chosen Auger spectra of the example alloy of Ni-Mo layers with polyethylene (Ni-Mo+PE) – 50 mA/cm² which contain main oxygen lines (KVV). We have observed characteristic line distortion which appears as an additional line (marked by A in Fig. 4) below the main line. According to the Cini model the main line is connected with the antibonding energy level, the additional line appear as consequence selfconvolutions (Coulomb correlations), and the bonding energy level has a small intensity [33, 34, 35]. Therefore we are recognized C-oxides, which depend on the interaction between carbon and oxygen.

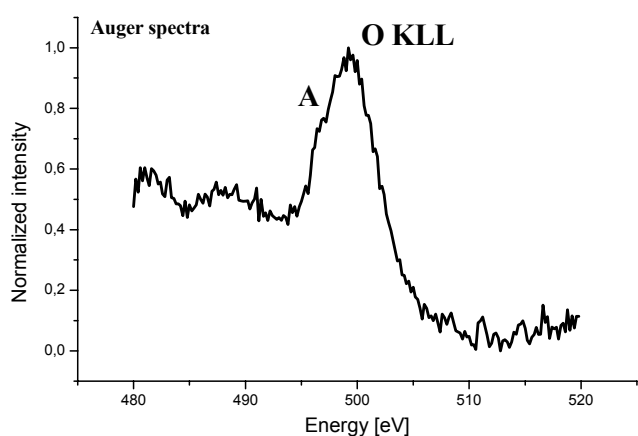


Fig. 4. Experimental shape of oxygen (KLL) and an additional (satellite peak A) Auger lines obtained for the Ni-Mo layers with polyethylene (Ni-Mo+PE) – 50 mA/cm².

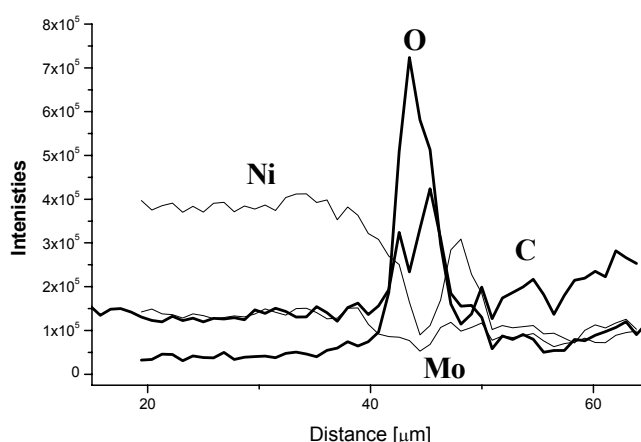


Fig. 5. Scan lines of the experimental intensities of the main Auger lines for elements Ni, O, Mo, and C obtained for Ni-Mo layers with polyethylene (Ni-Mo+PE) – 50 mA/cm².

The Fig. 5 presents the scan lines of the spectral intensities of the elements Ni, Mo, C, and O obtained for the same example alloy. The increase of carbon content accompanies the increase of oxygen content (and decrease of nickel and molybdenum contents) what evidences the polymere formation. So, the profile of these curves suggest that the polythiophene were electrodeposited in that sample. The similar results were obtained for other alloys as well.

4. Conclusions

- there are three ways of polymerization and layer deposition:
 - polythiophen + Ni-Mo – process of electropolymerization and Ni-Mo electrodeposition in the cathodic process.
 - polypyrrole + Ni-Mo – two-step process: electropolymerization in the anodic process and Ni-Mo electrodeposition in the cathodic process.
 - polyethylene + Ni-Mo – process of Ni-Mo electrodeposition with grains of polyethylene in the cathodic process.
- the values of unit cell parameters slightly depend on the values of potentials and current densities.
- crystallite size of the obtained layers is in a range of 5 – 6 nanometers.
- the presence of the polymers in the electrolyte hampers the deposition process of the solid solution molybdenum in nickel.
- the Auger spectra analysis verifies the presence of the polymers in studied alloys.

Acknowledgements

This work is financially supported by State Committee for Scientific Research (grant PBZ/KBN -3 - T08C - 02826).

References

- [1] E. Beltowska-Lehman, E. Chassaing, J. of Applied Electrochemistry, Iss 5, Vol. 27 (1997) 568.
- [2] Y. Zeng, S.W. Yao, X.Q. Cao, X.H. Huang, Z.Y. Zhong, H.T. Guo, Chinese Journal of Chemistry, Iss3, Vol. 15 (1997) 193.
- [3] J. Niedbała, M. Popczyk, A. Budniok, E. Łągiewka, 4th Kurt Schwabe Corrosion Symposium, Mechanisms of Corrosion Prevention Proceedings, Helsinki University of Technology, Espoo, Finland, 13-17 June (2004) 195.
- [4] M. Popczyk, J. Niedbała, A. Budniok, E. Łągiewka, 4th Kurt Schwabe Corrosion Symposium, Mechanisms of Corrosion Prevention Proceedings, Helsinki University of Technology, Espoo, Finland, 13-17 June (2004) 202.
- [5] J.M. Jakšić, M.V. Vojnovic, N.V. Krstajic, Electrochim. Acta, 45 (2000) 4151.
- [6] I. Zhitomirsky, Suf. En., 20(1) (2004) 43.
- [7] R. Rajagopalan, J.O. Iroh, Surf. Eng., 18 (2002) 59.
- [8] A.M. Fenelon, C.B. Breslin, Electrochim. Acta, 47 (2002) 4467.
- [9] G.S. Akundy, J.O. Iroh, Polymer, 42 (2001) 9665.
- [10] J. Niedbała, I. Napłoszek-Bilnik, A. Budniok, Acta Metall. Slov., 102 (2004) 220.
- [11] O. Ouerghi, A. Touhami, N. Jaffrezic-Renault, C. Martelet, H.B. Ouada, S. Cosnier, IEEE Sens.J., 4(5) (2004) 559.
- [12] M. Onoda, Y. Kato, H. Shonaka, K. Tada, Transaction of the Institute of Electrical Engineers of Japan, Part A, 124 A(2) (2004) 120.
- [13] C.T. Kou, T.R. Liou, Synth. Met., 82 (1996) 167.
- [14] M. Omastova, S. Kosina, J. Pionteck, A. Janke, J. Pavlinec, Synth. Met., 81 (1996) 49.
- [15] A. Bozkurt, U. Akbulut, L. Toppare, 82 (1996) 41.
- [16] H. Korri-Youssoufi, F. Garnier, P. Srivastava, P. Godillot, A. Yassar, J. Chem. Soc., 119 (1997) 7388.
- [17] M. Zhou, J. Heinze, Electrochim. Acta 44 (1999) 1733.
- [18] W. Su, J.O. Iroh, J. Appl. Polym. Sci., 65(30) (1997) 417.
- [19] F. Beck, R. Michaelis, F. Schloten, B. Zinger, Electrochim. Acta, 34 (1994) 229.
- [20] J.O. Iroh, W. Su, J. Appl. Polym. Sci., 71 (1999) 2075.
- [21] K.M. Cheung, D. Bloor, G.C. Stevens, Polymer Physic Group Conference, (1987) 9.
- [22] B. Sari, M. Talu, Synth. Met., 94 (1998) 221.
- [23] W. Su, J.O. Iroh, Electrochim. Acta, 44 (1999) 2173.
- [24] G. Torres-Gomez, P. Gomez-Romero, Synth. Met. 98 (1998) 95.
- [25] M.A. Malik, M.T. Gałkowski, H. Bala, B. Grzybowska, P.J. Kulesza, Electrochim. Acta, 44 (1999) 2157.
- [26] H. Hammache, L. Makhloufi, B. Saidani, Corr. Sci., 45 (2003) 2031.
- [27] Z. Abdel Hamid, I.M. Ghayad, Materials Letters, 53 (2002) 238.
- [28] M. Karolus, E. Łągiewka, Solid State Phenomena, Trans Tech. vol. 94 (2003) 217.
- [29] M. Karolus, E. Łągiewka, Proceedings of the XIX Conference on Applied Crystallography, Kraków 2003, 337.
- [30] M. Karolus, E. Łągiewka, Proceedings of the 12th International Scientific Conference Achievements in Mechanical & Materials Engineering, Zakopane 2003, 439-442.
- [31] M. Karolus, E. Łągiewka, Journal of Alloys and Compounds Vol. 367 Issues 1&2 (2004) 235.
- [32] G.K. Williamson and W.H. Hall, Acta Metall. 1 (1953) 22.
- [33] E. Rówiński, Surface Science, vol 411 (1998) 316.
- [34] E. Rówiński, E. Łągiewka, Vacuum, vol. 54 (1999) 37.
- [35] M. Cini, Solid State Communications, vol 20 (1976) 605.